Heliyon 5 (2019) e02031

Contents lists available at ScienceDirect

Heliyon

journal homepage: www.heliyon.com

Electrochemical detection of paracetamol and dopamine molecules using nano-particles of cobalt ferrite and manganese ferrite modified with graphite

Yogendra Kumar, Panchanan Pramanik, Dipak Kumar Das *

Department of Chemistry, GLA University, 17 Km Stone NH-19 Delhi Mathura Highway Chaumuhan, Mathura, 281406, India

ARTICLE INFO

Keywords:
Electrochemistry
Materials chemistry
Nano manganese ferrite
Nano cobalt ferrite
Paracetamol
Dopamine
Electrochemical analysis

ABSTRACT

Some electrodes for efficient detection of paracetamol and dopamine were developed from nano sized material of cobalt ferrite (np-$CoFe_2O_4$) and manganese ferrite (np-$MnFe_2O_4$). These oxides were synthesized by combustion method using cobalt nitrate, manganese acetate and ferric nitrate as precursors in the presence of sugar and ethanolamine. The crystallite size, shape and morphology of nano material were characterized by X-ray diffraction pattern (XRD), field emission scanning electron microscopy (FESEM) and energy-dispersive X-ray spectroscopy (EDS) techniques. The crystallite sizes of synthesized nano-particles (nps) were in the range from 10 to 12 nm (calculated using Debye-Scherrer equation) with cubic crystal system. These particles were utilized as electrode modified with graphite for simultaneous detection of paracetamol and dopamine through cyclic voltammetry and Differential pulse voltammetry techniques and was found to be superior to reported literatures. The minimum detection limit of paracetamol and dopamine at $CoFe_2O_4$/GP electrode were 250 nM and 350 nM while at $MnFe_2O_4$/GP electrode it was 300 nM and 400 nM, respectively. Both the electrodes exhibited the linearity range from3 μM to 200 μM & 3 μM–160 μM for paracetamol and 3 μM–180 μM & 5 μM to 200 for dopamine, respectively. Two oxidation peaks of paracetamol and dopamine were well separated in phosphate buffer (pH = 6) in mixture with 100 mVs^{-1} and 50 mVs^{-1} scan rate for cyclic voltammetry and Differential pulse voltammetry, respectively. Both the electrodes demonstrated satisfactory results in real samples of paracetamol and dopamine.

1. Introduction

For detection of drug molecules in bio-fluids, the drug monitoring is essential and can play an important role in drug quality control. Paracetamol (acetaminophen-N-acetyl-*p*-aminophenol, PCM), a well known antipyretic & analgesic compound is extensively used for the treatment of fever, cough & cold, pain including muscular ache, chronic pain, migraine, headache, backache and toothache [1, 2, 3]. PCM offers some protection against ovarian cancer [4] when the therapeutic doses are administered, without any harmful side effect but the overdose and the chronic use of PCM produces toxic metabolite accumulation which may result in kidney & liver failure or even death [5, 6, 7, 8].

Dopamine [4-(2-aminoethyle) benzene-1,2-diol, DA], a naturally occurring biogenic compound, known for its inhibitory neurotransmitter, is produced in the "Dargic neurons" in the ventral tegmental area (VTA) of the mid brain, strongly associated with reward mechanisms in the brain like memory, locomotion, learning and behavior of cognition. As a hormone, it mediates not only the functioning of central and peripheral nervous system [9, 10] during physical activities but also is responsible for emotion and endocrine system. Low concentration of DA may lead to burning mouth syndrome [11], restless leg syndrome [12], Senile dementia, fibromyalgia [13, 14] and rarely depression [15]. Depletion of DA in cerebral region may lead to Parkinson's disease [16] while high concentration of DA, due to addiction of cocaine, heroin, nicotine, alcohol and long term smoking etc., may act on sympathetic nervous system and cause abnormal blood pressure and an incensement in heart rate.

A large number of analytical techniques like titremetry [1], high performance liquid chromatography [17, 18, 19], spectrophotometry [20], chemiluminesence [21], gas-chromatography-mass spectrometry [22] and ultraviolet spectrophotometry [23] have been developed for the detection of PCM and DA in biological fluids and tablets. But these techniques are not convenient for routine analysis due to their tedious extraction process. Recently developed electrochemical techniques [24,

* Corresponding author.
E-mail address: deepak.das@gla.ac.in (D.K. Das).

https://doi.org/10.1016/j.heliyon.2019.e02031
Received 18 February 2019; Received in revised form 13 May 2019; Accepted 28 June 2019

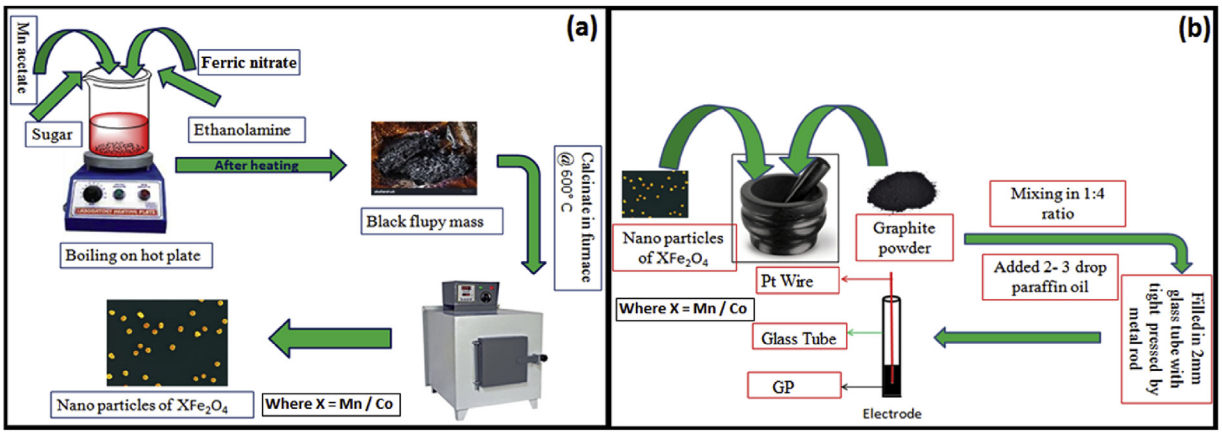

Fig. 1. (a) Schematic diagram for the synthesis of np-XFe_2O_4, (b) Preparation of electrode using synthesized nano-particles.

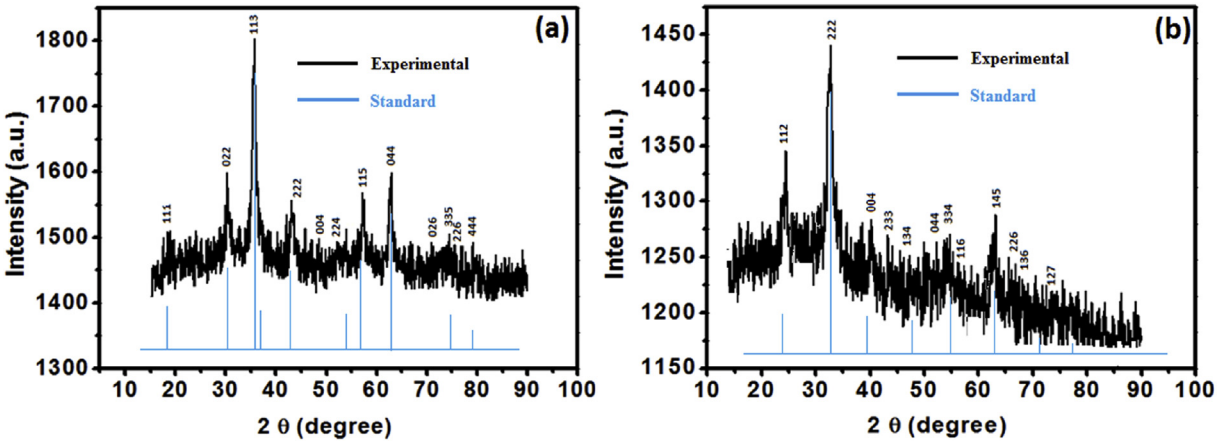

Fig. 2. XRD image of synthesized (a) np-$CoFe_2O_4$ and (b) np-$MnFe_2O_4$.

Table 1
Lattice parameters for the synthesized Manganese ferrite and Cobalt ferrite nano particles.

(a) For Manganese ferrite nano particles						
S.No	Standard values of a (Å)	Calculated value of a (Å)	Deviation	h	k	l
1	9.4000	9.4000	0.0000	2	2	2
2	9.4000	9.3999	0.0001	0	4	4
3	9.4000	9.3999	0.0001	2	2	6
(b) For Cobalt ferrite nano particles						
S.No	Standard values of a (Å)	Calculated value of a (Å)	Deviation	h	k	l
1	8.3410	8.3410	0.0000	1	1	3
2	8.3410	8.3410	0.0000	1	1	5
3	8.3410	8.3409	0.0001	0	4	4

*The systems are cubic so lattice parameters are equal (a = b = c).
The values of "**a**" are calculated from stronger peaks of XRD.

25, 26, 27, 28, 29, 30] have received tremendous attention for the detection of PCM and DA in bio fluids, due to their high selectivity, low cost, easy handling and less time consuming nature. Literature review reveals that nano materials with porous morphology having high surface area were conventionally used for electrode material for the detection of bio-molecules as well as drug molecules [31, 32, 33]. Various electrodes have been developed for detection of these molecules. The developed electrodes are gold nano particles for PCM [34], multi-walled carbon nano-tubes for PCM [35], nitrogen doped porous graphitic carbon for the detection of PCM [36], MWCNTs modified carbon paste electrode for DA [37], multi-walled carbon nano-tubes/graphene oxide nano-composite-modified glassy carbon electrode for DA and PCM [38], activated graphene-Nafion modified glassy carbon electrode for DA and acetaminophen [39], carbon paste electrode modified with 4-porphyrin for the simultaneous quantification of DA, acetaminophen-3 and tyrosine [40], glassy carbon electrode modified with a nano-composite consisting of nanoporous platinum-yttrium and graphene for DA [41], graphene ink film for PCM [47], F.D. Saccone synthesized $CoFe_2O_4$ nano particles by co-precipitation method using NaOH, but not used for electrochemical detection [42]. Zeid Abdullah Alothman et al. developed acid functionalized multi-wall carbon nano-tubes (f-MWCNTs) modified glassy carbon electrodes for the simultaneous determination of DA & PCM [43], G. P. Keeley et al. developed a sensor for simultaneous electrochemical determination of DA and PCM based on thin pyrolytic carbon films [44], Q Wan et al. developed MWNT-film coated electrodes for voltammetric detection of acetaminophen [45], S.F. Wang et al. developed Carbon-coated nickel magnetic nano-particles modified electrodes as a sensor for determination of acetaminophen [25], L. Fu et al. Graphene Ink Film Based Electrochemical Detector for Paracetamol [46].

No report is available on detection of PCM and DA simultaneously using npCoFe_2O_4/GPornpMnFe_2O_4/GP electrodes. Herein we report cheaper and effective electrodes from np-$CoFe_2O_4$ and np-$MnFe_2O_4$modified with graphite for the detection of PCM & DA. Both modified electrodes (np-$CoFe_2O_4$/GP & np-$MnFe_2O_4$/GP) have superior electrocatalytic activities for oxidation of PCM & DA separately as well as in

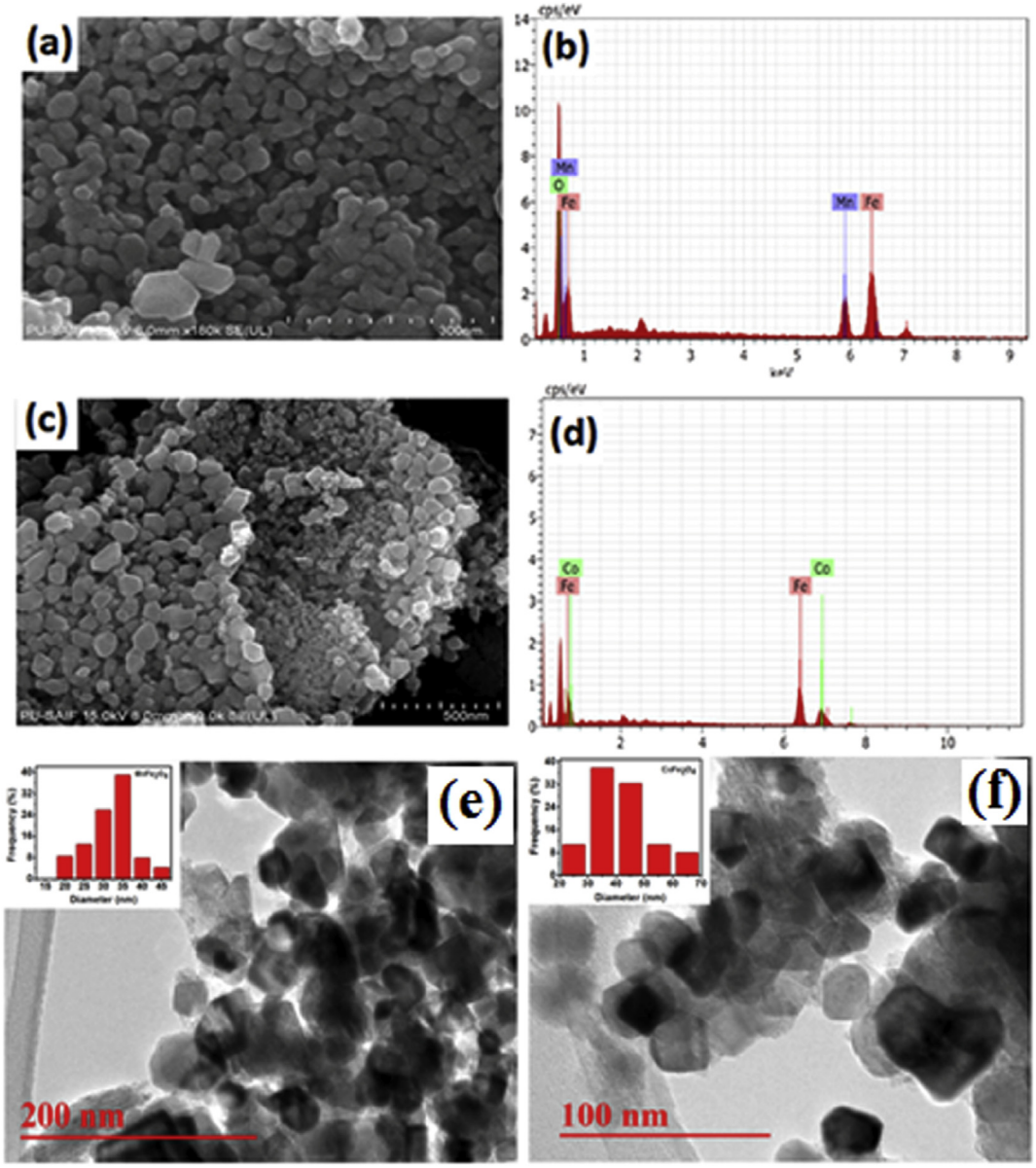

Fig. 3. FESEM image of (a) $MnFe_2O_4$ (c) $CoFe_2O_4$ and EDS image of (b) $MnFe_2O_4$ and (d) $CoFe_2O_4$ nps, TEM image of synthesized particles (e) for $MnFe_2O_4$, (f) for $CoFe_2O_4$ and inset of Fig. 3 (e) and (f) represents particle size distribution graphs of $MnFe_2O_4$ and $CoFeO_4$ respectively.

the mixture with good selectivity, high sensitivity and better repeatability. These electrodes also displayed efficient performance for real samples of commercially available PCM.

2. Experimental

2.1. Chemical and reagents

Manganese acetate [$Mn(CH_3COO)_2$], Cobalt nitrate ($Co(NO_3)_2{\cdot}6H_2O$), Monoethanolamine (C_2H_7NO), Nitric Acid (HNO_3), sugar and Paraffin oil were purchased from Merck, India, graphite flakes was obtained from Sigma Aldrich, USA. All the reagents were of analytical grade and used without further purification. Double distilled water was used for preparation of all the solutions.

2.2. Synthesis of nano particles

To the aq. solution of manganese acetate (0.01 mol) and Ferric nitrate (0.02 mol), added monoethanolamine (0.25 mol) and sugar (0.17 mol) followed by addtion of HNO_3 (0.44 mol) with constant strring. The

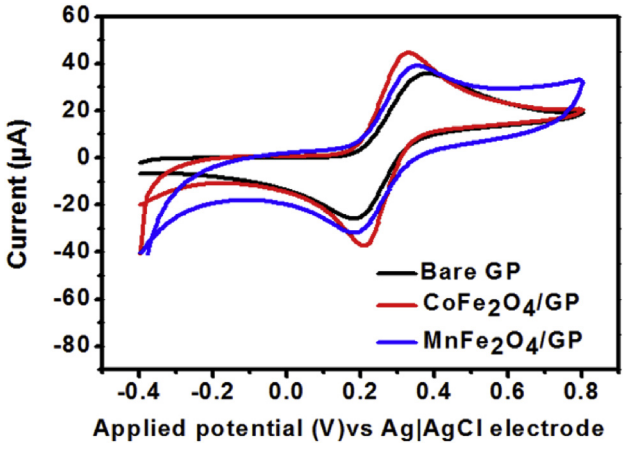

Fig. 4. Cyclic Voltammogram obtained for 3.0 mM $Fe(CN)_6^{-4}$ at $CoFe_2O_4$/GP, $MnFe_2O_4$/GP and bare GP electrodes at 100 $mVsec^{-1}$ scan rate with phosphate buffer solution of pH 6.0.

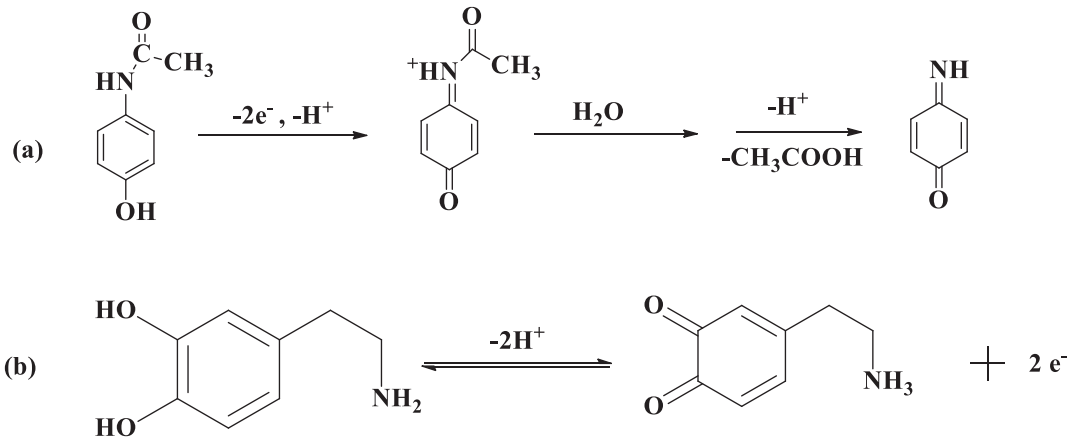

Suggested oxidation mechanisms (a) for paracetamol and (b) for dopamine at prepared electrode

Scheme 1. Suggest oxidation mechanism for analyte molecule at prepared electrode.

mixture was then boiled on a hot plate until a black fluffy mass was obtained. Further, this fluffy mass was calcined in muffle furnace at 600 °C for about 6–7 h to obtain the nanoparticles of $MnFe_2O_4$. We also adopted similar procedure by taking cobalt nitrate (0.01 mol) and ferric nitrate (0.02 mol), as a precursor material for the synthesis of $CoFe_2O_4$ nano particles (Fig. 1a).

2.3. Praparation of electrode

Synthesized np- $MnFe_2O_4$ and graphite powder in 1:4 (w/w) ratio were grinded along with 2–3 drop paraffin oil. The final paste was transferred into the capillary glass tube (2 mm inner diameter, 0.031 cm^2 geometrical surface area) and compressed with a metal rod. From the back side of the

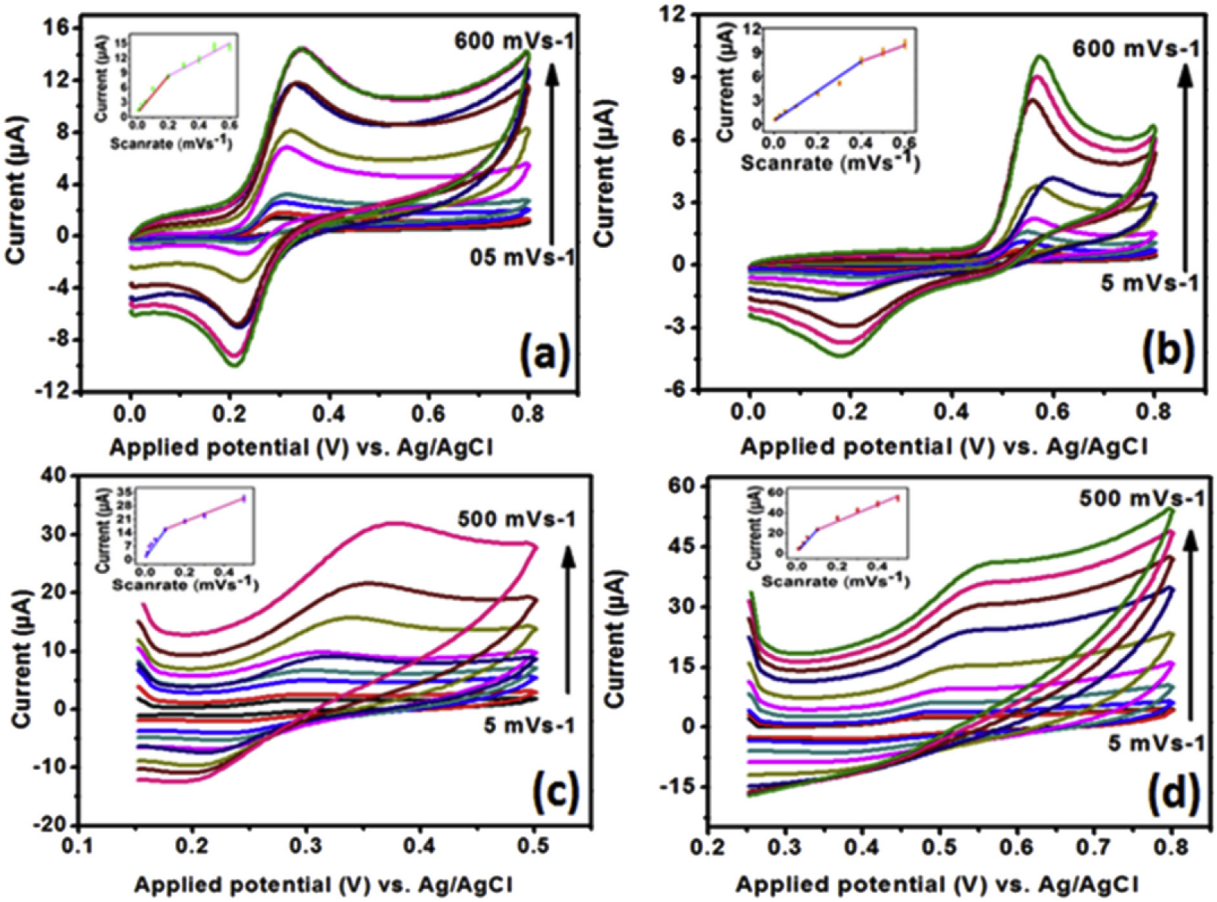

Fig. 5. Scan rate of 0.1 mM (a) DA varied at $CoFe_2O_4$/GP (b) PCM varied at $CoFe_2O_4$/GP electrode (c) DA varied at $MnFe_2O_4$/GP (d) PCM varied at $MnFe_2O_4$/GP electrode.

capillary tube, a Pt-wire was attached for electrical contact. Similar procedure was applied for the preparation of bare graphite paste electrode. 0.3 mM and 0.05 mM Al_2O_3 slurry was used to clean the surface of the electrodes. The electrodes were rinsed with ethanol and dried under N_2 atmosphere before experiments. Similar procedure was used for the preparation of $CoFe_2O_4$/GP electrode (Fig. 1b).

2.4. Apparatus and measurements

The crystallite size of synthesized nano material were determined by X-ray diffraction (XRD) patterns by Panalytical X-ray diffractometer, model no. X'PertPRO (Neertherlands) with Cu K-alpha radiation (λ = 1.5406Å). The morphology, shape, size and elemental composition of synthesized nano-particles were determined by Hitachi field emission scanning electron microscopy (FESEM), model no. SU8010 along with Bruker's energy-dispersive X-ray spectroscopy detector (EDS) model is XFlash 6130. TEM analysis was performed by FEI Tecnai G2 30 S-TWIN Model TEM microscope. All the electrochemical measurements were performed using AUTOLAB potentiostate/Galvanstate 101 (Netherlands) with three electrode system including a platinum electrode as a counter electrode and Ag/AgCl electrode as a reference electrode. All the electrochemical studies were carried out in 0.1(M) phosphate buffer of pH 6.0 at 25±2 °C using Cyclic voltammetery (CV) and Differential pulse voltammetry (DPV) techniques. All the CV measurements were carried out at a scan rate 100 mVs^{-1} but for DPV scan rate was maintained at 50 mVs^{-1}. DPV measurements were carried out with 5 mV step potential, 40 mV modulation amplitude, 0.02 s modulation times and 0.1 s interval time. The voltage ranges for the oxidation of DA and PCM in CV experiments were 0.25 V–0.35 V and 0.55V to 0.65 V, respectively. For DPV experiments with DA and PCM, voltage ranges were from 0.22 V to 0.3 V and 0.42 V–0.60 V, respectively.

3. Results and discussion

3.1. XRD analysis of $MnFe_2O_4$&$CoFe_2O_4$ nano-particles

XRD technique is used to get information about crystal structure and phase purity of the synthesized nano materials. Diffraction lines of XRD pattern were in good agreement with standard ICSD card No. 98-007-7782 for $CoFe_2O_4$ and ICSD card No. 98-001-7884 for $MnFe_2O_4$. The crystallite size of synthesized np-$MnFe_2O_4$ and np-$CoFe_2O_4$ were calculated using 'Debye–Scherrer method' ($D = K\lambda/\beta \cos\theta$), where D is average crystallite size, β is full width at half maxima (FWHM), λ is wavelength of X-rays (λ = 1.5406Å), θ is diffraction angle, and k is a constant value which depends on several factors including the Miller index [47] with selecting the 100% intensity peak with hkl value 113 for $CoFe_2O_4$ nps and also 100 % intensity peak with hkl value 222 for $MnFe_2O_4$ nps (see hkl value 113 in Fig. 2a and hkl value 222 in Fig. 2b.) The calculated crystallite sizes (D) of np-manganese ferrite and np-cobalt ferrite were found to be in ranges from 7 to 10 nm and 9–12 nm, respectively with cubic crystal system (Fig. 2). The lattice parameters are calculated and presented in Table 1.

3.2. FESEM, EDS and TEM analysis of $CoFe_2O_4$ & $MnFe_2O_4$ nano particles

The field emission scanning electron microscopy (FESEM) technique was used to study the surface morphologies of synthesized cobalt ferrite

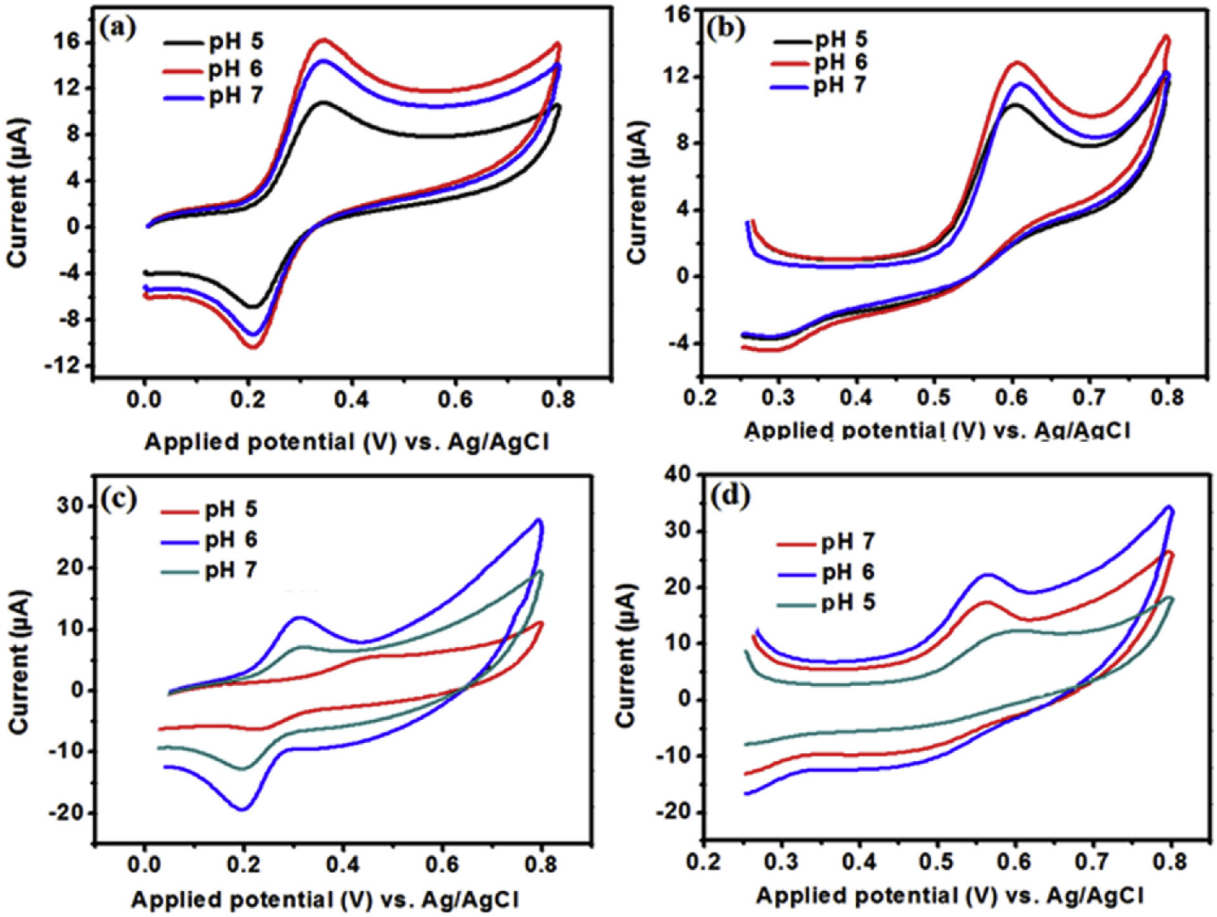

Fig. 6. pH variation *vs* current plot in PBS from pH 5 to pH 7 (a) at $CoFe_2O_4$/GP electrode in 0.1 mM DA solution (b) at $CoFe_2O_4$/GP electrode in 0.1 mM PCM solution (c) at $MnFe_2O_4$/GP electrode in 0.1 mM DA solution (d) at $MnFe_2O_4$/GP electrode in 0.1 mM PCM solution.

Table 2
Electrocatalytic oxidation of individual and binary mixture of bio-molecules (PCM and DA) at $CoFe_2O_4$/GP and bare GP electrodes by using cyclic voltammetry at scan rate 100 mV/s.

Electrodes	Concentration (μM)		Anodic peak potential (mV)		Oxidation peak current (μA)	
	PCM	DA	PCM	DA	PCM	DA
$CoFe_2O_4$/GP	100	0	597	-	11.73	
GP	100	0	610	-	5.24	
$CoFe_2O_4$/GP	0	100	-	337	-	14.52
GP	0	100	-	453	-	3.04
$CoFe_2O_4$/GP	50	50	673	431	9.16	7.91

(np-$CoFe_2O_4$) and manganese ferrite (np-$MnFe_2O_4$). Fig. 3 illustrates that the particles have uniform cubic structural morphology with narrow size distribution. The EDS image of synthesized nano-particles Fig. 3(b)and 3(d) show that nano-particles had no impurities. The TEM studies (fig. 3 e and 3 f) of synthesized nano materials (cobalt ferrite and manganese ferrite) also supported the FESEM results.

3.3. *Electrochemical studies of $MnFe_2O_4$/GP and $CoFe_2O_4$/GP electrodes*

Electrochemical properties of prepared $MnFe_2O_4$/GP electrode, $CoFe_2O_4$/GP electrode and bare GP electrodes were studied by using standard redox system $[Fe(CN)_6]^{-4}/[Fe(CN)_6]^{-3}$ as reference. The comparative cyclic voltammograms of 3 mM $K_4[Fe(CN)_6]$ solution at bare GP, $MnFe_2O_4$/GP and $CoFe_2O_4$/GP electrodes are represented in Fig. 4. In this study, approximately two protons were transferred in the reaction. Paracetamol oxidation is a two-electron and two-proton process (Scheme 1) [48].

Some parameters like particle size, surface defects, electrochemical band gap, composition, optical band gap & capping ligand play important roles in the voltammetric response of the semiconducting materials [49, 50, 51, 52, 53]. For these reasons nano-particles are very relevant for electro-chemical analysis. From Fig. 4 it was noted that the peak potential separation (ΔEp) at $MnFe_2O_4$/GP and $CoFe_2O_4$/GP electrodes were 156 mV and 116 mV, respectively whereas at bare GP electrode it was 185 mV. According to Velasco equation the low value of ΔEp indicates the faster electron transfer between the electrode surface and analyte molecules. From the comparison of ΔEp of prepared electrodes, it can be concluded that np-$MnFe_2O_4$/GP and np-$CoFe_2O_4$/GP electrodes are efficient for electron transfer than bare GP. As per cyclic voltametric response for DA, the oxidation peak currents at $CoFe_2O_4$/GP and $MnFe_2O_4$/GP were found to be 4.58 and 2.27 times higher with respect to bare GP. For PCM oxidation peak current was about 4.5 times higher with respect to bare GP at $CoFe_2O_4$/GP electrode. The peak separations of detecting molecules (one peak for DA and another for PCM) had been found to be 220 mV and 216 mV at $CoFe_2O_4$/GP electrode and $MnFe_2O_4$/GP electrode, respectively.

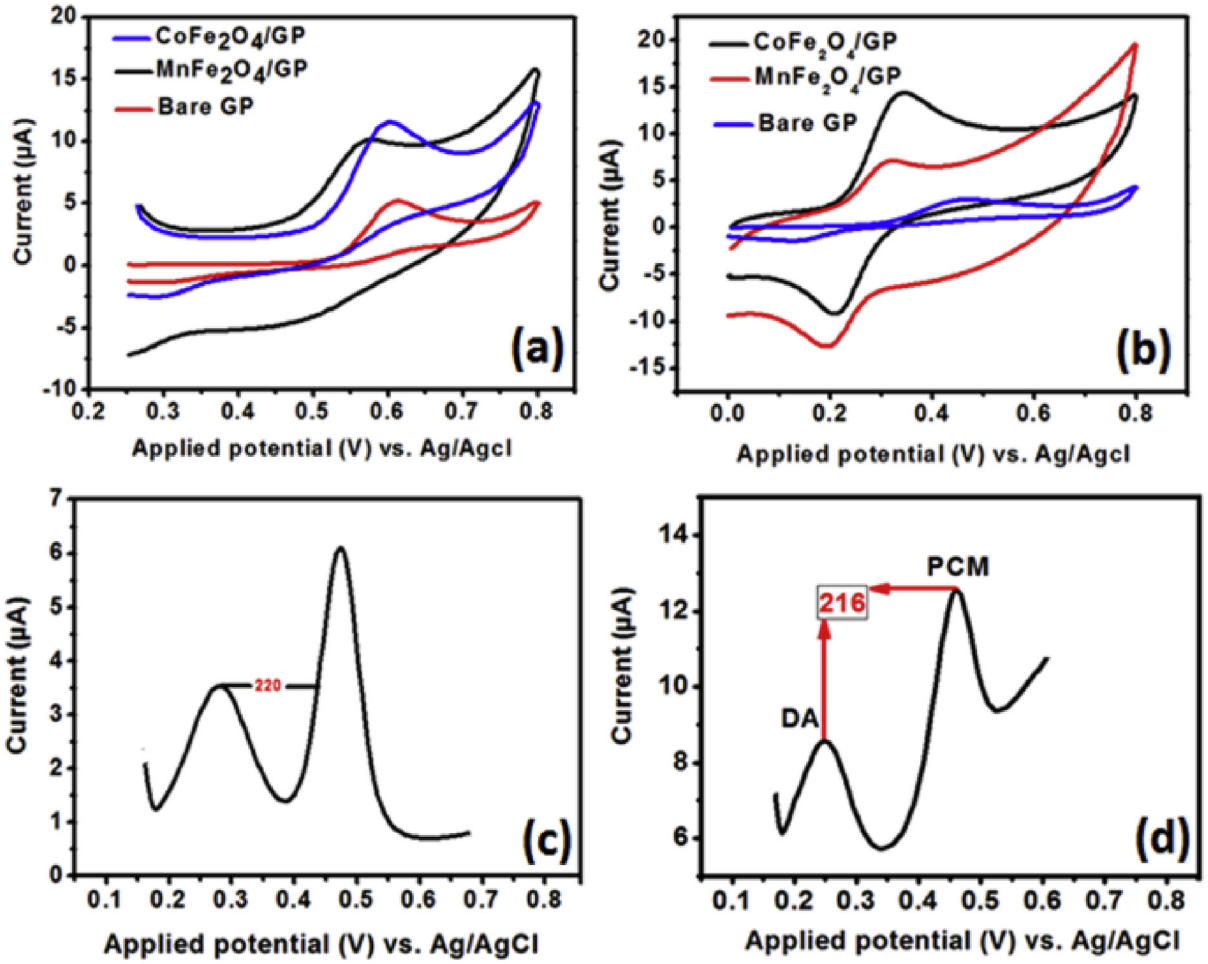

Fig. 7. CV plots of (a) 0.1 mM PCM at both npCoFe$_2$O$_4$/GP, npMnFe$_2$O$_4$/GP electrodes and at bare GP electrode (b) 0.1 mM DA at both npCoFe$_2$O$_4$/GP, npMnFe$_2$O$_4$/GP electrodes and at bare GP electrode (c) DPV plot in mixture of 0.1 mM PCM and 0.1 mM DA of at npCoFe$_2$O$_4$/GP electrodes (d) DPV plot in mixture of 0.1 mM PCM and 0.1 mM DA of at npMnFe$_2$O$_4$/GP electrodes in 0.1M phosphate buffer pH 6.0 for CV, scan rate 100 mVs^{-1} and for DPV, scan rate 50 mVs^{-1}.

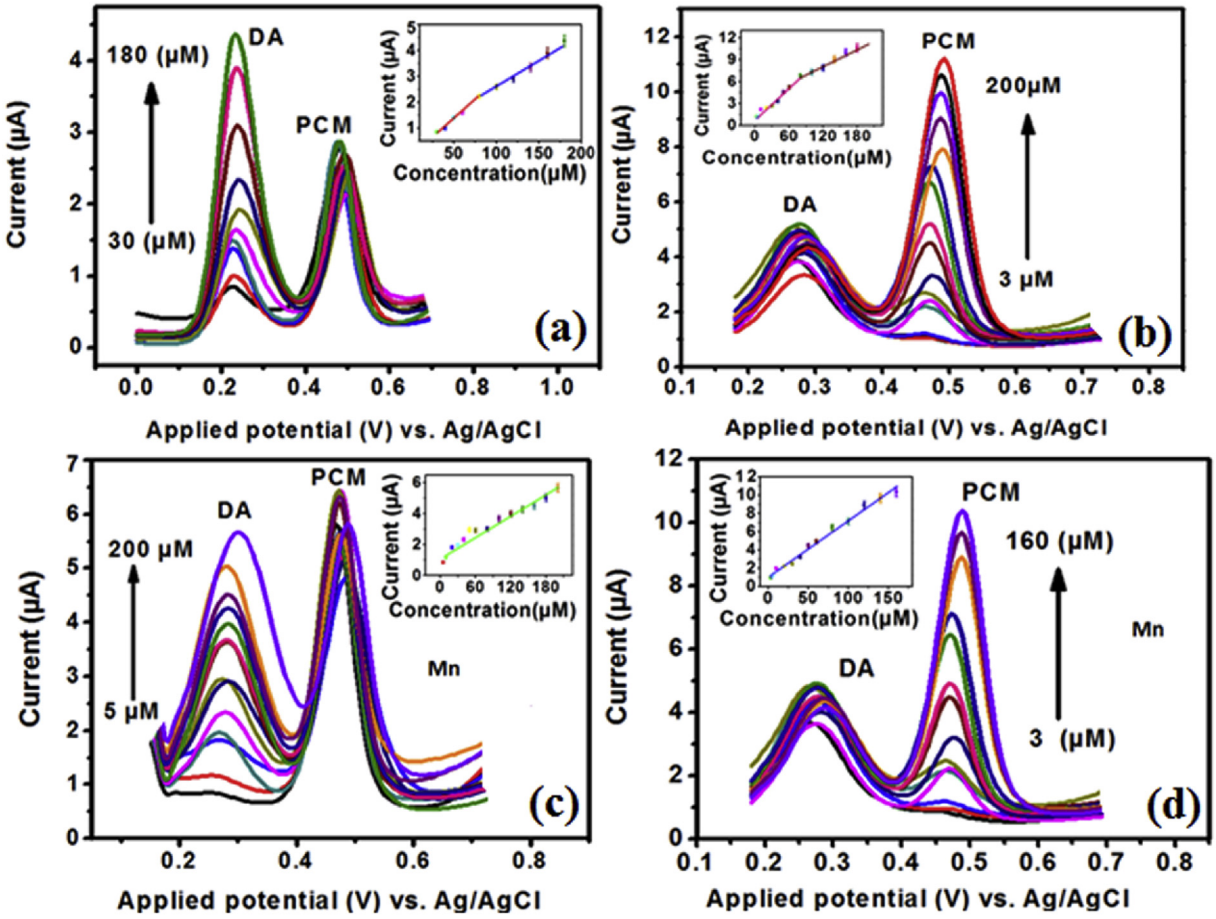

Fig. 8. DPV in mixture (a) PCM containing 100 μM and different concentration of DA from 3, 5, 10, 20, 30, 40, 50, 60, 80, 100, 120, 140, 160, and 180 μM (b) DA containing 100 μM and different concentration of PCM 3, 4, 5, 10, 20, 30, 40, 50, 60, 80, 100, 120, 140, 160, 180 and 200 μM at $CoFe_2O_4$/GP electrode (c) PCM containing 100 μM and different concentration of DA: 5, 10, 20, 30, 40, 50, 60, 80, 100, 120, 140, 160, 180 and 200 μM (d) DA containing 100 μM and different concentration of PCM 3, 4, 5, 10, 20, 30, 40, 50, 60, 80, 100, 120, 140 and 160 μM at $MnFe_2O_4$/GP electrode in 0.1M phosphate buffer pH 6.0.

3.4. Effect of the scan rate and pH on the oxidation of DA & PCM

Effects of scan rates towards the electrocatalytic oxidation of DA and PCM were investigated with the scan rates from 5 mVs^{-1} to 500 mVs^{-1} in CV technique. It was noted that there was a linear increment in the peak current for both the molecules with increase of scan rate. Fig. 5 indicates the oxidation process was diffusion controlled at the surface of electrodes. The pH of supporting electrolyte plays a key role for the electrochemical oxidation of molecules. To study the effect of pH on the oxidation of DA and PCM, 0.1 M phosphate buffer solution (PBS) were used having pH range from 5.0 to 7.0. The peak currents of DA and PCM increased with increasing the pH up to 6.0 and then decreased with further increase of pH value. The maximum peak current value at npXFe_2O_4/GP (where X is Co/Mn) was observed at pH 6.0. The results are shown in Fig. 6. So PBS of pH 6.0 was used for all experimental works.

3.5. Electrocatalytic oxidation of PCM and DA at np$CoFe_2O_4$/GP and np$MnFe_2O_4$/GP electrodes

Electro-catalytic behavior of modified electrodes had been studied in CV and DPV techniques for individual molecule and mixture. The results of np-$MnFe_2O_4$/Gp electrode, np-$CoFe_2O_4$/GP electrode and bare GP electrode are shown in Fig. 6. Electrochemical measurement parameters are summarized in Table 2. The cyclic voltammogram of individual PCM molecule at bare GP electrode, np-$MnFe_2O_4$/GP electrode and np-$CoFe_2O_4$/GP electrodes are also shown in Fig. 7 (a) and for DA in Fig. 7 (b).

Both the molecules (PCM & DA) followed irreversible oxidation characters at all the electrodes. For DA, oxidation peak potential at bare GP electrode was 365 mV while at$MnFe_2O_4$/GP and $CoFe_2O_4$/GP electrodes, oxidation peak potential were 345 mV and 342 mV, respectively. For PCM oxidation peak potential at bare GP was 613 mV while at$MnFe_2O_4$/GP and $CoFe_2O_4$/GP electrodes the oxidation peak potential was 567mV and 602 mV, respectively. The electrodes np-$MnFe_2O_4$/GP and np-$CoFe_2O_4$/GPacted as efficient sensors for both the molecules. Fig.7(c) and 7(d) present well separated DPV plots of binary mixture of DA and PCM molecules. At $CoFe_2O_4$/GP electrode, oxidation peak for PCM appeared at 470 mV and for DA, it appeared at 250 mV and separation is 220 mV. While at $MnFe_2O_4$/GP electrode oxidation peak for PCM appeared at 480 mV and for DA, it appeared at 264 mV with the separation 216 mV.

3.6. Simultaneous determination of PCM & DA

For the simultaneous determination of DA & PCM molecules in the mixture was verified by CV technique maintaining voltage range from 0.2 V to 0.85 V with the scan rate 100 mV/s. For better resolution and higher peak current, differential Pulse Voltammertry (DPV) was preferred. A controlled DPV experiment had been carried out at $CoFe_2O_4$/GP electrode, keeping concentration of PCM (100 μM) fixed, with variable concentration of DA from 3 to 180 μM (Fig. 8a). The first linear range were observed from 30 to 80 μM having corresponding regression equation IDA $y = 0.000 + 0.021$ $R^2 = 0.978$ and second linear range was from 80 to 180

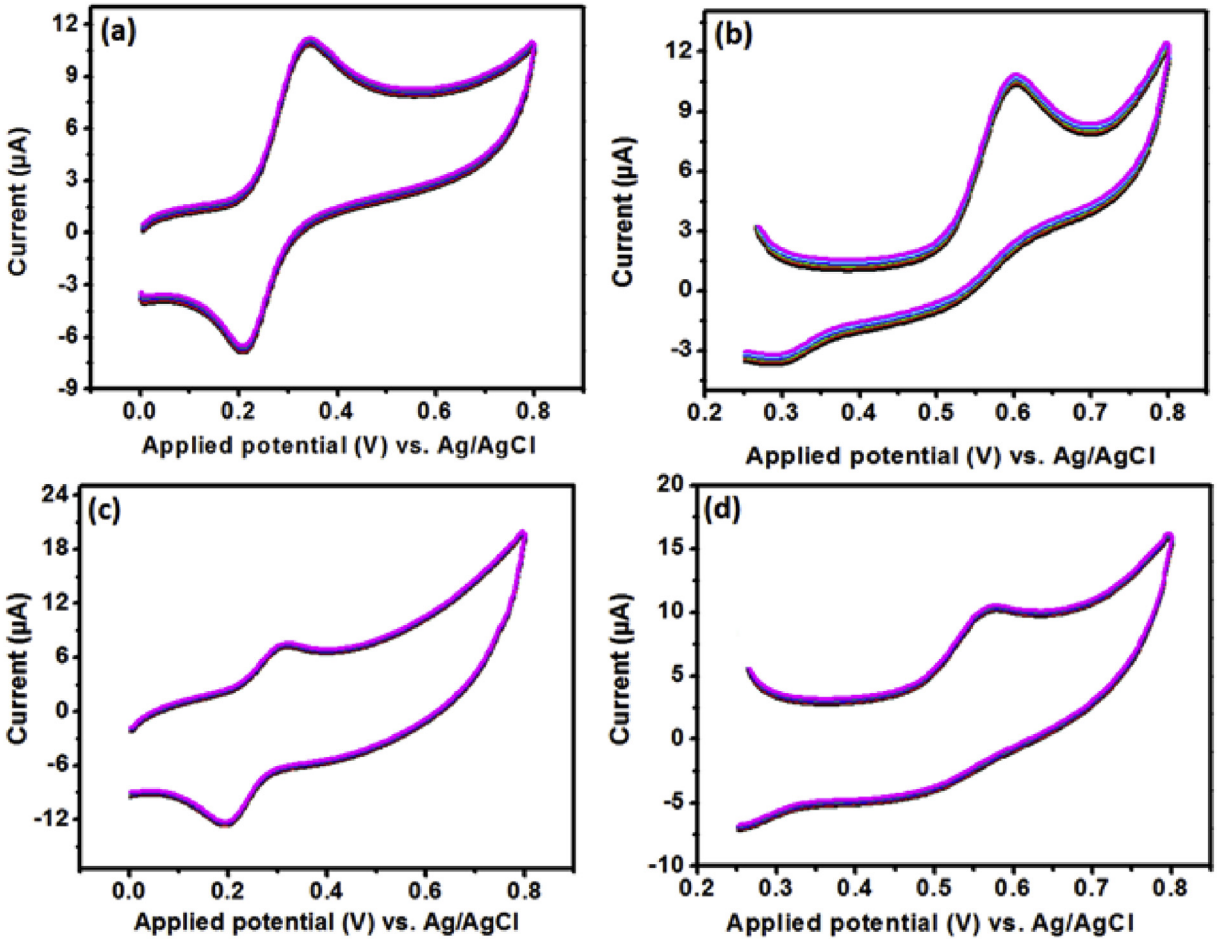

Fig. 9. Five successive DPV measurements at $CoFe_2O_4$/GP electrode (a) for DA and (b) for PCM and at $MnFe_2O_4$/GP electrode in (c) for DA and (d) for PCM in 0.1 mM solution with PBS pH 6.0 buffer solution as a supporting electrolyte.

μM having corresponding regression equation IDA y = 0.001–0.069, R^2 = 0.988. Similar experiment had been carried out keeping concentration of DA (100 μM) fixed with variable concentration of PCM from 3 to 200 μM (Fig. 8 b). The first linear range was observed from 3 to 80 μM with corresponding regression equation I_{PCM} y = 0.07 + 0.946, R^2 = 0.978 and second linear range was observed from 80 to 200 μM with corresponding regression equation I_{PCM} y = 0.002 + 0.172, R^2 = 0.989. At $CoFe_2O_4$/GP electrode two liner ranges was observed. The first linear range might have appeared due to adsorption of DA/PCM molecule on the surface of the sensor electrode, while second liner range might be due to diffusion processes on the monolayer covered surface [54].

The similar experiment at $MnFe_2O_4$/GP electrode had been performed keeping concentration of PCM (100 μM) fixed with variable concentration of DA from 5 to 200 μM and observed linearity range from 5 to 200 μM with corresponding regression equation y = 0.003DA+0.049 R^2 = 0.99 (Fig. 8c). Keeping concentration of DA (100 μM) fixed, in similar experiment, with variable concentration of PCM from 3 to 160 μM, it was observed linearity from 3 to 160 μM with corresponding regression equation y = 0.001PCM+0.065 R^2 = 0.961 (Fig. 8d).

At np$CoFe_2O_4$/GP electrode, the minimum detection limit was observed 250 nM and 350 nM for PCM and DA respectively and at np$MnFe_2O_4$/GP electrodes it was 300 nM and 400 nM, respectively for above molecules.

3.7. Comparative study of different synthesized modified electrodes with present electrodes

On the basis of comparison (Table 3), it may be concluded that the newly developed np-manganese ferrite and np-cobalt ferrite modified graphite paste electrode are superior to previous reports in sensitivity i.e. linearity range and minimum detection limit.

3.8. Repeatability, stability and reproducibility of electrodes

To check stability of the modified electrodes (XFe_2O_4/GP, where X = Co & Mn), electrodes were stored at 30 °C ± 1 °C for 90 days and observed 97% retention of sensing response indicating good stability of the electrodes. The electrode responses were noted for 15 consecutive measurements and were found to have similar performance indicating good repeatability. To check reproducibility, five electrodes were prepared. All five electrodes showed similar results supporting good reproducibility. All the experiments concluded that the reproducibility, repeatability and stability of the electrode were excellent

Table 3
Comparison of sensitivity of manganese-ferrite and cobalt ferrite modified graphite paste electrodes with other previously developed electrodes.

Modified Electrode	detection limit (nM)		Liner range (μM)		Ref.
	PCM	DA	PCM	DA	
f-MWCNT	600	800	3–300	3–200	[43]
Pyrolytic carbon	1400	2300	15–225	18–270	[44]
MWNTs/GCE	2400	NA	5–100	NA	[45]
CCNMnps	600	NA	NA	NA	[25]
GI/GCE	2700	NA	10–500	NA	[46]
$CoFe_2O_4$/GP	250	350	3–200	3–180	Our work
$MnFe_2O_4$/GP	300	400	3–160	5–200	Our Work

Table 4
Determination of PCM and DA in real samples with modified electrodes (n = 1) XFe_2O_4/GP nps where X = Co and Mn.

Electrode	Sample	Original/Diluted sample (μM)	Spiking (μM)	Found (μM)	R.S.D[1] (%)	Recovery[2] (%)
XFe_2O_4/GPnps	**Urine Sample**					
	DA	20	30	50.5	1.92	101.5
	PCM	0	50	50.1	1.54	100.1
	Commercial available					
	PCM	20	30	49.8	1.4	99.7

[1] Relative standard deviation.

[2] $\text{Recovery} = \frac{\text{Found}(\mu M)\text{-Diluted biologicalfluids/pharmaceuticalsample}(\mu M)}{\text{Spiking}(\mu M)} \times 100$

(Fig. 9).

3.9. Real sample analysis

The performance of the modified electrodes was checked using real samples of drug molecules using urine, PCM tablets & injections. The recovery values for PCM in tablet and injection were 98.3%, 99.7% respectively with respect to standard sample. The collection of urine sample was done after 5 h of PCM dose. It was diluted with phosphate buffer solution (0.1M) of pH 6. The results are summarized in Table 4. From the results it may be concluded that the np-XFe_2O_4/GP (where X = Mn and Co) electrodes have good efficiency for the analysis of PCM & DA in real samples.

4. Conclusion

Nano particles of $CoFe_2O_4$ and $MnFe_2O_4$ were synthesized using combustion technique having crystallite size of 10–12 nm. The synthesized nano-particle based electrodes demonstrated excellent sensitivity in detecting drug/bio molecules (PCM and DA) in biological fluids and commercial samples with the minimum detection limit 0.25 μM and 0.35 μM, respectively at np-$CoFe_2O_4$/GP electrode and 0.30 μM and 0.40 μM, respectively at np-$MnFe_2O_4$/GP electrode.

Declarations

Author contribution statement

Yogendra Kumar: Performed the experiments; Contributed reagents, materials, analysis tools or data.

Panchanan Pramanik: Analyzed and interpreted the data.

Dipak Das: Conceived and designed the experiments; Wrote the paper.

Funding statement

This work was supported by the management of GLA University, Mathura (India).

Competing interest statement

The authors declare no conflict of interest.

Additional information

No additional information is available for this paper.

References

[1] R.M.D. Carvalho, R.S. Freire, S. Rath, L.T. Kubota, Effects of EDTA on signal stability during electrochemical detection of acetaminophen, J. Pharm. Biomed. Anal. 34 (2004) 871–878.

[2] R.T. Kachoosangi, G.G. Wildgoose, R.G. Compton, Sensitive adsorptive stripping voltammetric determination of PCM at multiwalled carbon nanotube modified basal plane pyrolytic graphite electrode, Anal. Chim. Acta 618 (2008) 54–60.

[3] R.N. Goyal, V.K. Gupta, M. Oyama, N. Bachheti, Differential pulse voltammetric determination of PCM at nanogold modified indium tin oxide electrode, Electrochem. Commun. 7 (2005) 803–807.

[4] D.W. Cramer, B.L. Harlow, L.T. Ernstoff, K. Bohlke, W.R. Welch, E.R. Greenberg, Over-the-counter analgesics and risk of ovarian cancer, Lancet 351 (1998) 104–107.

[5] R.N. Goyal, A.R. Rana, M.A. Aziz, d. M. Oyama, Effect of gold nanoparticle attached multi-walled carbon nano tube-layered indium tin oxide in monitoring the effect of PCM on therelease of epinephrine, Anal. Chim. Acta 693 (2011) 35–40.

[6] Y. Fan, J.H. Liu, H.T. Lu, Q. Zhang, Electrochemical behavior and voltammetric determination of PCM on Nafion/TiO2–graphene modified glassy carbon electrode, Colloids Surf., B 85 (2011) 289–292.

[7] R.N. Goyal, V.K. Gupta, S. Chatterjee, Voltammetric biosensors for the determination of PCM at carbon nanotube modified pyrolytic graphite electrode, Sens. Actuators, B 149 (2010) 252–258.

[8] J.B. Raoof, M. Baghayeri, R. Ojani, A high sensitive voltammetric sensor for qualitative and quantitative determination of phenobarbital as an antiepileptic drug in presence of cetaminophen, Colloids Surf., B 95 (2012) 121–128.

[9] R.A. Wise, DA, learning and motivation, Nat. Rev. Neurosci. 5 (2004) 483–494.

[10] G.A. Evtugyn, R.V. Shamagsumova, R.R. Sitdikov, I.I. Stoikov, I.S. Antipin, M.V. Ageeva, T. Hianik, Dopamine sensor based on a composite of silver nanoparticles implemented in the electroactive matrix of calixarenes, Electroanalysis 23 (2011) 2281–2289.

[11] P.B. Wood, P. Schweinhardt, E. Jaeger, A. Dagher, H. Hakyemez, E.A. Rabiner, M.C. Bushnell, B.A. Chizh, Fibromyalgia patients show an abnormal dopamine response to pain, Eur. J. Neurosci. 25 (2007) 3576–3582.

[12] S. Cervenka, S.E. Palhagen, R.A. Comley, G. Panagiotidis, Z. Cselenyi, J.C. Matthews, R.Y. Lai, C. Halldin, L. Farde, Support for dopaminergic hypoactivity in restless legs syndrome: a PET study on D2-receptor binding, Brain 129 (2006) 2017–2028.

[13] Z. Dursun, B. Gelmez, Simultaneous Determination of Ascorbic Acid, Dopamine and uric acid at Pt nanoparticles decorated multiwall carbon nanotubes modified GCE, Electroanalysis 22 (2010) 1106–1114.

[14] Z. Yang, X. Huang, J. Li, Y. Zhang, S. Yu, Q. Xu, X. Hu, Carbon nanotubes-functionalized urchin-like In_2S_3 nanostructure for sensitive and selective electrochemical sensing of dopamine Microchim, Acta 177 (2012) 381–387.

[15] S.H. Kollins, R.A. Adcock, ADHD, Altered dopamine neurotransmission, and disrupted reinforcement processes: implications for smoking and nicotine dependence, Prog. Neuro Psychopharmacol. 52 (2014) 70–78.

[16] M.E.J. Rice, Ascorbate regulation and its neuroprotective role in the brain, Trends Neurosci. 23 (2000) 209–216.

[17] L.S. Jensen, J. Valentine, R.W. Milne, A.M. Evans, The quantification of paracetamol, paracetamol glucuronide and paracetamol sulphate in plasma and urine using a single high-performance liquid chromatography assay, J. Pharm. Biomed. Anal. 34 (2004) 585–593.

[18] C. Nebot, S.W. Gibb, K.G. Boyd, Quantification of human pharmaceuticals in water samples by high performance liquid chromatography–tandem mass spectrometry, Anal. Chim. Acta 598 (2007) 87–94.

[19] I. Baranowska, P. Markowski, J. Baranowski, Simultaneous determination of 11 drugs belonging to four different groups in human urine samples by reversed-phase high-performance liquid chromatography method, Anal. Chim. Acta 570 (2006) 46–58.

[20] A.R. Sirajuddin, A. Khaskheli, M.I. Shah, A. Bhanger, S. Niaz, Mahesar,Simpler spectrophotometric assay of paracetamol in tablets and urine samples, Spectrochim. Acta, Part A 68 (2007) 747–751.

[21] D. Easwaramoorthy, Y.C. Yu, H.J. Huang, Chemiluminescence detection of paracetamol by a luminol-permanganate based reaction, Anal. Chim. Acta 439 (2001) 95–100.

[22] D.J. Speed, S.J. Dickson, E.R. Cairns, N.D. Kim, Analysis of paracetamol using solid-phase extraction, deuterated internal standards, and gas chromatography–mass spectrometry, J. Anal. Toxicol. 25 (2001) 198–202.

[23] M.V.N.K. Talluri, M.K. Bairwa, H.H.T. Dugga, R. Srinivas, Development and validation of RP-HPLC and ultraviolet spectrophotometric methods of analysis for simultaneous determination of paracetamol and lornoxicam in pharmaceutical dosage forms, J. Liq. Chromatogr. Relat. Technol. 35 (2012) 129–140.

[24] J. Chen, P. He, H. Bai, S. He, T. Zhang, X. Zhang, F. Dong, Poly(β-cyclodextrin)/carbon quantum dots modified glassy carbon electrode: preparation, characterization and simultaneous electrochemical determination of dopamine, uric acid and tryptophan, Sens. Actuators, B 252 (2017) 9–16.
[25] S.F. Wang, F.R. Xie, F. Hu, Carbon-coated nickel magnetic nanoparticles modified electrodes as a sensor for determination of acetaminophen, Sens. Actuators, B 123 (2007) 495–500.
[26] R.N. Goyal, S.P. Singh, Voltammetric determination of paracetamol at C60-modified glassy carbon electrode, Electrochim. Acta 51 (2006) 3008–3012.
[27] I. Baranowska, M. Koper, The preliminary studies of electrochemical behavior of paracetamol and its metabolites on glassy carbon electrode by voltammetric methods, Electroanalysis 21 (2009) 1194–1199.
[28] B. Saraswathyamma, I. Grzybowska, C. Orlewska, J. Radecki, W. Dehaen, K.G. Kumar, H. Radecka, Electroactive dipyrromethene-Cu(II) monolayers deposited onto gold electrodes for voltammetric determination of paracetamol, Electroanalysis 20 (2008) 2317–2323.
[29] J. Huang, Q. Zeng, S. Bai, L. Wang, Application of coal in electrochemical sensing, Anal. Chem. 89 (16) (2017) 8358–8365.
[30] J. Huang, G. Yue, J. Yang, S. Bai, Q. Hu, L. Wang, Design, synthesis and application of carboxylic multi-walled carbon nanotubes/tetrahexahedral platinum nanocrystals nanocomposites biosensor for simultaneous determination of guanine and adenine in DNA, J Electroanal Chem801 (2017) 536–544.
[31] S. Pradhan, S. Biswas, D.K. Das, R. Bhar, R. Bandyopadhyay, P. Pramanik, An efficient electrode for simultaneous determination of guanine and adenine using nanosized lead telluride with grapheme, New J. Chem. 42 (2018) 564–573.
[32] S. Pradhan, R. Das, S. Biswas, D.K. Das, R. Bhar, R. Bandyopadhyay, P. Pramanik, Chemical synthesis of nanoparticles of nickel telluride and cobalt telluride and its electrochemical applications for determination of uric acid and adenine, Electrochimi, Acta 238 (2017) 185–193.
[33] Y. Kumar, S. Pradhan, S. Pramanik, R. Bandhyopadhyay, D.K. Das, P. Pramanik, Efficient electrochemical detection of guanine, uric acid and their mixture by composite of nano-particles of lanthanides ortho-ferrite XFeO3 (X= La, Gd, Pr, Dy, Sm, Ce and Tb), J. Electroanal. Chem. 830 (2018) 95–105.
[34] N.F. Atta, A. Galal, S.M. Azab, Electrochemical determination of paracetamol using gold nanoparticles – application in tablets and human fluids, Int. J. Electrochem. Sci. 6 (2011) 5082–5096.
[35] J. Hui, W. Li, Y. Guo, Z. Yang, Y. Wang, C. Yu, Electrochemical sensor for sensitive detection of paracetamol based on novel multi-walled carbon nanotubes-derived organic–inorganic material Bioprocess, Biosyst. Eng. 37 (2014) 461–468.
[36] S. Biswas, D. Chakraborty, R. Das, R. Bandyopadhyay, P. Pramanik, A simple synthesis of nitrogen doped porous graphitic carbon:Electrochemical determination of PCM in presence of ascorbic acid and p-aminophenol, Anal. Chim. Acta 890 (2015) 98–107.
[37] J.B. Raoof, , 1, A. Kiani, R. Ojani, R. Valiollahi, Electrochemical determination of dopamine using banana-MWCNTs modified carbon paste electrode, Anal. Bioanal. Electrochem. 3 (2011) 59–66.
[38] C. Srikanth, P. Selvakumar, M. Veerappan, S.M. Chen, Simultaneous electrochemical determination of dopamine and paracetamol on multiwalled carbon nanotubes/graphene oxide nanocomposite-modified glassy carbon electrode, Talanta 117 (2013) 297–304.
[39] K. Dongwon, L. Sohee, P. Yuanzhe, Electrochemical determination of dopamine and acetaminophen using activated graphene-Nafion modified glassy carbon electrode, J. Electroanal. Chem. 794 (2017) 221–228.
[40] J.C.K. Mbouguen, E. Ngameni, Simultaneous quantification of dopamine, acetaminophen and tyrosine at carbon paste electrode modified with porphyrin and clay, Anal. Methods 9 (2017) 4157–4166.
[41] D. Chen, C. Tian1, X. Li1, Z. Li1, Z. Han1, C. Zhai1, Y. Quan, R.C.G. Zhang, Electrochemical determination of dopamine using a glassy carbon electrode modified with a nanocomposite consisting of nanoporous platinum-yttrium and grapheme, Microchim Acta 185 (2018) 98.
[42] F.D. Saccone, S. Ferrari, D. Errandonea, F. Grinblat, V. Bilovol, S. Agouram, Cobalt ferrite nanoparticles under high pressure, J. Appl. Phys. 118 (7) (2015), 075903.
[43] Z.A. Alothman, N. Bukhari, S.M. Wabaidur, S. Haider, Simultaneous electrochemical determination of DA and acetaminophen using multiwall carbon nanotubes modified glassy carbon electrode, Sens. Actuators, B 146 (2010) 314–320.
[44] G.P. Keeley, N. McEvoy, H. Nolan, S. Kumar, E. Rezvani, M. Holzinger, S. Cosnier, G.S. Duesberg, Simultaneous electrochemical determination of DA and PCM based on thin pyrolytic carbon films, Anal. Methods 4 (2012) 2048–2053.
[45] Q. Wan, X. Wang, F. Yu, X. Wang, N. Yang, Effects of capacitance and resistance of MWNT-film coated electrodes on voltammetric detection of acetaminophen, J. Appl. Electrochem. 39 (2009) 1145–1151.
[46] L. Fu, K. Xie, Y. Zheng, L. Zhang, W. Su, Graphene ink film based electrochemical detector for paracetamol analysis, Electronics 7 (2) (2018) 15.
[47] B.D. Cullity, S.R. Stock, Elements of X-ray Diffraction Boston, Addison-Wesley, MA, USA, 2001.
[48] M. Zidan, T.W. Tee, A. Abdullah, Z. Zaina, G.J. Kheng, Electrochemical oxidation of paracetamol mediated by nanoparticlesbismuth oxide modified glassy carbon electrode, Int. J. Electrochem. Sci. 6 (2011) 279–288.
[49] S.K. Haram, B.M. Quinn, A.J. Bard, Electrochemistry of CdS Nanoparticles: a correlation between optical and electrochemical band gaps, J. Am. Chem. Soc. 123 (2001) 8860–8861.
[50] C. Querner, P. Reiss, S. Sadki, M. Zagorska, A. Pron, Size and ligand effects on the electrochemical and spectroelectrochemical responses of CdSe nanocrystals, Phys. Chem. Chem. Phys. 7 (2005) 3204–3209.
[51] N. Gaponik, S.K. Poznyak, N.P. Osipovich, A. Shavel, A. Eychmuller, Electrochemical probing of thiol-capped nanocrystals, Microchim. Acta 160 (2008) 324–327.
[52] H.Z. Zhong, S.S. Lo, T. Mirkovic, Y.C. Li, Y.Q. Ding, Y.F. Li, G.D. Scholes, Noninjection gram-scale synthesis of monodisperse pyramidal CuInS2 nanocrystals and their size-dependent properties, ACS Nano 4 (2010) 5253–5262.
[53] S.N. Inamdar, P.P. Ingole, S.K. Haram, Determination of band structure parameters and the quasi-particle gap of CdSe quantum dots by cyclic voltammetry, ChemPhysChem 9 (2008) 2574–2579.
[54] Y. Fana, K.J. Huanga, D.J. Niua, C.P. Yang, Q.S. Jing, TiO2-graphene nanocomposite for electrochemical sensing of adenine and guanine, Electrochim. Acta 56 (2011) 4685–4690.